



Tract shape modelling provides evidence of topological change in corpus callosum genu during normal ageing

Mark E. Bastin^{a,b,*}, Jakub P. Piatkowski^c, Amos J. Storkey^d, Laura J. Brown^e,
Alasdair M.J. MacLullich^{b,e}, Jonathan D. Clayden^{c,f}

^a Medical and Radiological Sciences (Medical Physics), University of Edinburgh, UK

^b MRC Centre for Cognitive Ageing and Cognitive Epidemiology, University of Edinburgh, UK

^c Neuroinformatics Doctoral Training Centre, University of Edinburgh, UK

^d Institute for Adaptive and Neural Computation, University of Edinburgh, UK

^e Geriatric Medicine, University of Edinburgh, UK

^f Institute of Child Health, University College London, UK

ARTICLE INFO

Article history:

Received 3 April 2008

Received 22 May 2008

Accepted 23 June 2008

Available online 18 July 2008

Keywords:

Ageing

White matter

Magnetic resonance imaging

Water diffusion tensor

Tractography

ABSTRACT

Understanding how ageing affects brain structure is an important challenge for medical science. By allowing segmentation of fasciculi-of-interest from diffusion magnetic resonance imaging (dMRI) data, tractography provides a promising tool for assessing white matter connectivity in old age. However, the output from tractography algorithms is usually strongly dependent on the subjective location of user-specified seed points, with the result that it can be both difficult and time consuming to identify the same tract reliably in cross-sectional studies. Here we investigate whether a novel method for automatic single seed point placement based on tract shape modelling, termed probabilistic model-based neighbourhood tractography (PNT), can reliably segment the same tract from subject to subject in a non-demented cohort aged over 65 years. For the fasciculi investigated (genu and splenium of corpus callosum, cingulum cingulate gyri, corticospinal tracts and uncinate fasciculi), PNT was able to provide anatomically plausible representations of the tract in question in 70 to 90% of subjects compared with 2.5 to 60% if single seed points were simply transferred directly from standard to native space. In corpus callosum genu there was a significant negative correlation between a PNT-derived measure of tract shape similarity to a young brain reference tract and age, and a trend towards a significant negative correlation between tract-averaged fractional anisotropy and age; results that are consistent with previous dMRI studies of normal ageing. These data show that it is possible automatically to segment comparable tracts in the brains of older subjects using single seed point tractography, if the seed point is carefully chosen.

© 2008 Elsevier Inc. All rights reserved.

Introduction

There is increasing evidence for a progressive loss of myelin and axonal membrane integrity in normal ageing (Bartzokis et al., 2003; Armstrong et al., 2004). This reduction in white matter microstructural integrity can be investigated using diffusion magnetic resonance imaging (dMRI), which measures the random macroscopic motion of water molecules within brain tissue. Fitting the diffusion tensor (DT) model to the diffusion-weighted signals obtained from a dMRI experiment permits the determination of two parameters, the mean diffusivity ($\langle D \rangle$) and fractional anisotropy (FA) (Pierpaoli et al., 1996). These scalar indices measure the magnitude and directional coherence of water molecule diffusion *in vivo*, and provide useful biomarkers for probing white matter structure. Those DT-MRI studies

that have investigated white matter structure in normal ageing, typically using region-of-interest (ROI) or histogram analysis, have found that $\langle D \rangle$ increases while FA decreases with age, an observation consistent with a gradual microstructural deterioration in white matter coherence (for a review see Sullivan and Pfefferbaum, 2006). However, it still remains unclear as to whether this reduction in white matter integrity selectively and differentially affects frontal lobes, the so-called 'frontal ageing' hypothesis (O'Sullivan et al., 2001; Head et al., 2004; Pfefferbaum et al., 2005; Sullivan et al., 2006), or whether changes are more widespread leading to a more global disconnection syndrome (Geschwind, 1965; Greenwood, 2000).

By allowing segmentation of specific tracts-of-interest from dMRI data, tractography provides a promising tool for further assessing the affects of age on white matter connectivity (Sullivan et al., 2006). However, this promise is tempered by the fact that the output from tractography algorithms is usually strongly dependent on the potentially subjective location of user-specified 'seed points', with the result that it can be both difficult and time consuming to identify reliably the

* Corresponding author. Western General Hospital, Crewe Road, Edinburgh, EH4 2XU, UK. Fax: +440 131 537 1026.

E-mail address: Mark.Bastin@ed.ac.uk (M.E. Bastin).

same tract from subject to subject (Ciccarelli et al., 2003; Heiervang et al., 2006; Wakana et al., 2007). This problem can be addressed using the multiple ROI approach where the tractography algorithm is initiated from a seed region within the fasciculus-of-interest and constrained by one or more ‘waypoint’ ROIs through which the resulting streamlines must pass. While this method can generate reproducible tracts (Conturo et al., 1999; Heiervang et al., 2006; Wakana et al., 2007), it does require the user to define these waypoint ROIs, a condition that imposes a strong a priori restriction on the tractography output. It also implicitly assumes that single seed points are insufficient to segment tracts reproducibly.

We have shown, however, that it is possible to segment the same fasciculus in groups of young subjects from single seed point tractography output, if that seed point is chosen carefully. In this generic method, which we term neighbourhood tractography (NT), seed points are automatically placed in a neighbourhood surrounding a seed point transferred from standard space, with the tract that best matches a predefined reference tract in terms of both length and shape chosen from this group of ‘candidate’ tracts (Clayden et al., 2006). Recently, we have developed a formal probabilistic tract shape modelling approach to NT, in which the inter-subject variability in tract shape and length are explicitly represented using probability distributions (Clayden et al., 2007). Training data are created separately from the reference tract and employed to estimate parameters of the tract model. Candidate tracts can then be evaluated for similarity to the reference tract under the model, and an absolute goodness-of-match measure can be calculated in terms of a log-ratio of likelihoods. This measure gives a sense of the extent of topological difference between the reference and candidate tracts, relative to the variability found among the training data. While this new approach, which we term probabilistic model-based NT (PNT), has been shown to segment reliably different tracts in young healthy brains (Clayden et al., 2007), to be clinically useful, its performance needs to be evaluated in a wider range of populations.

In the current work, we investigate whether PNT can reliably segment comparable tracts in ageing subjects with varying degrees of brain atrophy in a cohort of non-demented subjects aged over 65 years. This is achieved by comparing the number of anatomically acceptable tracts generated by PNT with the simple, but automatic, approach of transferring single seed points directly from standard to the subject’s native space for eight fasciculi-of-interest and calculating the inter-subject coefficients-of-variation (CV) for the resulting tract-averaged $\langle D \rangle$ and FA measurements. The PNT-derived tract-averaged diffusion parameters are then correlated with age to explore whether white matter structure is affected in normal ageing. We also use the log-ratio measure derived from the tract shape models to explore topological changes associated with ageing. Before presenting these data, however, we briefly outline the PNT method, full details of which can be found in Clayden et al. (2007).

Materials and methods

Tract shape modelling

PNT, which has no specific dependence on the type of tractography algorithm used to generate the underlying connectivity data, works on the principle that two equivalent tracts are expected to have similar shape and length. Thus, given a predefined reference tract which is taken to epitomise the fasciculus-of-interest, and a series of candidate tracts generated from a set of single seed points, the ‘best’ seed point is that which produces the tract that has the closest shape and length match to the reference.

Each tract is represented for matching purposes in terms of a uniform cubic B-spline curve. Such a curve can be created from a set of streamlines produced by a tractography algorithm, by first calculating a median streamline, and then fitting the curve to that path. Associated with a B-spline is a set of so-called ‘knot points’ or simply

‘knots’, which for our purposes are equally spaced along the curve, such that one of them falls on the original seed point. The vectors linking successive knot points therefore form a reasonable approximation to the trajectory of the tract.

Fig. 1 shows parts of two tracts, a reference and a candidate, represented in terms of their knot points and inter-knot vectors. Each tract is notionally split into ‘left’ and ‘right’ parts, separated by the seed point, which is indicated with a ringed knot. The ‘left length’, L_1 , is the number of knots on the left side of the tract, and likewise for the ‘right length’, L_2 . To characterise shape, the model uses the angles between equivalent inter-knot vectors in the two tracts: these are denoted ϕ_u , where u indicates position in the tract such that it is negative on the left side and positive on the right. The model characterises the cosines,

$$S_u = \cos \phi_u, \quad (1)$$

of these ‘similarity angles’ rather than the angles themselves.

Given a data set, D , describing all of the candidate tracts, PNT calculates the probability that each candidate, indexed by i , represents the best available match, denoted m , to the reference tract. This is achieved using

$$P(m = i|D) \propto P(L_1^i | L_1^*) P(L_2^i | L_2^*) \prod_{u=1}^{\min\{L_1^i, L_1^*\}} P(s_{-u}^i) \prod_{u=1}^{\min\{L_2^i, L_2^*\}} P(s_u^i), \quad (2)$$

where L_1^* and L_2^* are the left and right lengths of the reference tract. The constant of proportionality in Eq. (2) is given by normalising over all values of i . The distributions over the similarity cosines are modelled with beta distributions, and regularised multinomial distributions are used to model the lengths, subject to a maximum length cut-off. It is the parameters of these distributions that are fitted, using the maximum likelihood method, from the training data. (Eq. (2) represents a slightly simpler tract shape model than that used in Clayden et al. (2007), since it ignores the continuity properties of the candidate tract beyond the end of the reference. This simplifies the model fitting process substantially without affecting the ability of the model to establish a match to the reference tract. Its use of the reference tract is, however, the same.)

For segmentation, the candidate seed point that a posteriori generates the best-matching tract to the predefined reference is determined as follows: (i) the tractography algorithm is run to generate a set of streamlines for each candidate seed point, (ii) the candidate median streamline is calculated and transformed into the space of the reference tract, (iii) a cubic B-spline is fit to the median streamline of the candidate tract using the knot spacing chosen for the reference tract, (iv) the similarity angles are calculated for the inter-knot vectors as shown in Fig. 1, (v) the right hand side of Eq. (2) is evaluated using length and angle distributions fitted from appropriately chosen training data, and the seed point which produces the highest matching probability is identified.

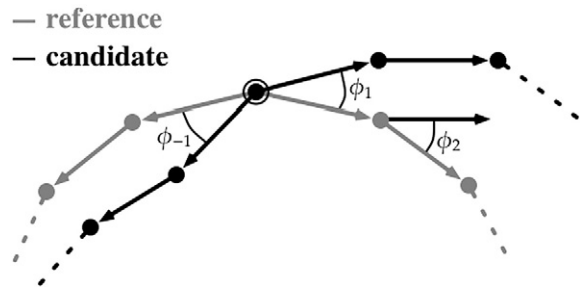


Fig. 1. Illustration of the similarity angles (ϕ) in the tract shape model. The filled circles represent successive knot points in the reference and candidate tracts. The ringed knot is the seed point, which is common to the two tracts. The second inter-knot vector from the candidate tract is shown connected to the reference tract knot point for illustration.

Finally, a measure of the absolute goodness-of-fit of the best match tract in any given test subject is provided by the log-ratio, R , between the matching likelihood (the right hand side of Eq. (2)) of the chosen candidate tract, and the matching likelihood of the reference tract to itself. Since the reference tract has, by definition, a log-ratio of zero, R will be negative for all other tracts; and the more negative it is, the less good is the fit between the reference and best match tract (see Fig. 2).

Subjects

Forty volunteers aged over 65 years (28 male; mean age 75.9 ± 4.9 years), without history of stroke or other neurological disorder, were recruited from the community. No subject had dementia as determined by a comprehensive neuropsychological assessment that included the Mini-Mental State Examination, and tests of memory and executive function. All were living independently and none had contraindications to MRI. Reference tract and model training data were obtained from fifteen younger healthy volunteers (8 male; mean age 31.5 ± 8.1 years). The study was approved by the Scotland A Research Ethics Committee and informed consent was obtained from each subject.

MRI protocol

All MRI data were collected using a GE Signa LX 1.5 T (General Electric, Milwaukee, WI, USA) clinical scanner equipped with a self-shielding gradient set (33 mT/m maximum gradient strength) and manufacturer supplied 'birdcage' quadrature head coil. The MRI examination comprised standard structural T_1 - and T_2 -weighted imaging, and a whole brain dMRI protocol based on single-shot, spin-echo, echo-planar (EP) imaging. The dMRI protocol consisted of 7 T_2 -weighted and sets of diffusion-weighted ($b = 1000$ s/mm²) axial EP volumes acquired with diffusion gradients applied in 64 non-collinear directions (Jones et al., 2002). Fifty-three contiguous slice locations were imaged with a field of view of 240×240 mm, an acquisition matrix of 96×96 (zero filled to 128×128) and a slice thickness of 2.5 mm, giving an acquisition voxel dimension of $2.5 \times 2.5 \times 2.5$ mm. The repetition and echo times for each EP volume were 13.5 s and 75 ms.

Image analysis

All DICOM format magnitude images were transferred from the scanner to a Dell Precision 690 workstation (Dell Computers, Round Rock, TX, USA) and converted into Analyze format (Mayo Foundation, Rochester, MN, USA).

Using tools freely available in FSL (FMRIB, Oxford, UK; <http://www.fmrib.ox.ac.uk>), the dMRI data were pre-processed to extract the brain, and bulk patient motion and eddy current induced artefacts removed by registering the diffusion-weighted to the first T_2 -weighted EP volume for each subject (Jenkinson and Smith, 2001). From these MRI data, $\langle D \rangle$ and FA volumes were generated for every subject in Analyze format using DTIFIT. The BEDPOST/ProbTrack algorithm was run with its default parameters, 5000 probabilistic

streamlines for each tract with a fixed separation distance of 0.5 mm between successive points, to generate the underlying connectivity data (Behrens et al., 2003).

Reference tracts and model training data

For this study, the fasciculi-of-interest were the genu and splenium of corpus callosum, cingulum cingulate gyri (CCG; Wakana et al., 2007), left and right projections of the pyramidal or corticospinal tract (CST), and uncinate fasciculi. These tracts were chosen because they have well known anatomy (see, for example, the white matter tractography atlases available at <http://cmrm.med.jhmi.edu>; Hua et al., 2008), and to provide both frontal and non-frontal tracts for comparison.

For each fasciculus, reference tracts were created from the tractography output produced from the subject of median age in the training group: a 31 year old female. Starting from initial Montréal Neurological Institute (MNI) coordinates located in the centre of each fasciculus in the standard brain (Evans et al., 2003), $[0, 28, 2]$ (genu), $[0, -38, 10]$ (splenium), $[\pm 8, -6, 36]$ (right and left CCG), $[\pm 22, -10, 10]$ (right and left CST) and $[\pm 32, 5, -10]$ (right and left uncinate fasciculi), tracts were generated by seeding within a $7 \times 7 \times 7$ neighbourhood centred at the points in the reference subject's native space corresponding to these standard brain coordinates. From the tractography output, and aided by a radiologist, eight reference tracts were chosen to epitomise each fasciculus-of-interest. The native space seed coordinates that produced these reference tracts were then transferred back to standard space to provide the reference tract MNI coordinates. Fig. 3 shows the reference tracts for genu, splenium, and right CCG, CST and uncinate fasciculus generated from seed points placed at the MNI coordinates indicated in Table 1.

A similar process was applied to the 14 remaining subjects in the training group, in order to generate sets of tracts with which to train the tract shape models. This was achieved by seeding in a $7 \times 7 \times 7$ neighbourhood centred at the reference tract MNI coordinate for each fasciculus-of-interest and choosing by hand the tract which matched the appropriate reference tract as closely as possible. Using this training data, the model parameters were fit using maximum likelihood (Clayden et al., 2007), thereby capturing the shape and length variation amongst the training tracts. Once the model had been trained, PNT was run over a neighbourhood of $7 \times 7 \times 7$ voxels again centred on the reference tract MNI coordinates for the ageing subjects. For each subject, the seed point that produced the best match tract to the reference was determined, with the resulting tractography mask thresholded at a connectivity value of 50 streamlines (1%) to exclude voxels with a very low probability of connection. This tract mask was binarized and then applied to each subject's $\langle D \rangle$ and FA volumes, and tract-averaged diffusion parameters determined. In all cases, median streamlines and B-splines were calculated as described in Clayden et al. (2007), being transformed into the space of the reference tract using FLIRT (Jenkinson and Smith, 2001). The process of calculating median streamlines, generating B-splines, training tract shape models and identifying the best match tract were implemented in R, an interpreted statistics and data analysis language (<http://www.r-project.org>).

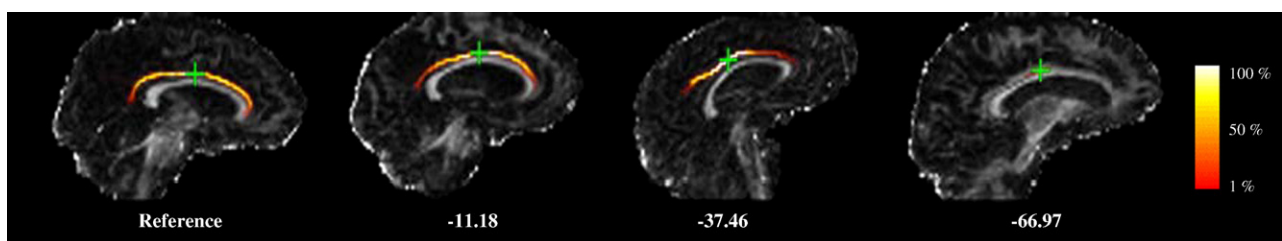


Fig. 2. Log-ratios between the matching likelihoods of the right cingulum cingulate gyri shown and the matching likelihood of the reference tract (R). As the fit between the best match tract and the reference worsens, R becomes increasingly negative. The colours represent the proportion of probabilistic streamlines generated from the seed point (green star) passing through each voxel, as indicated by the colour bar.

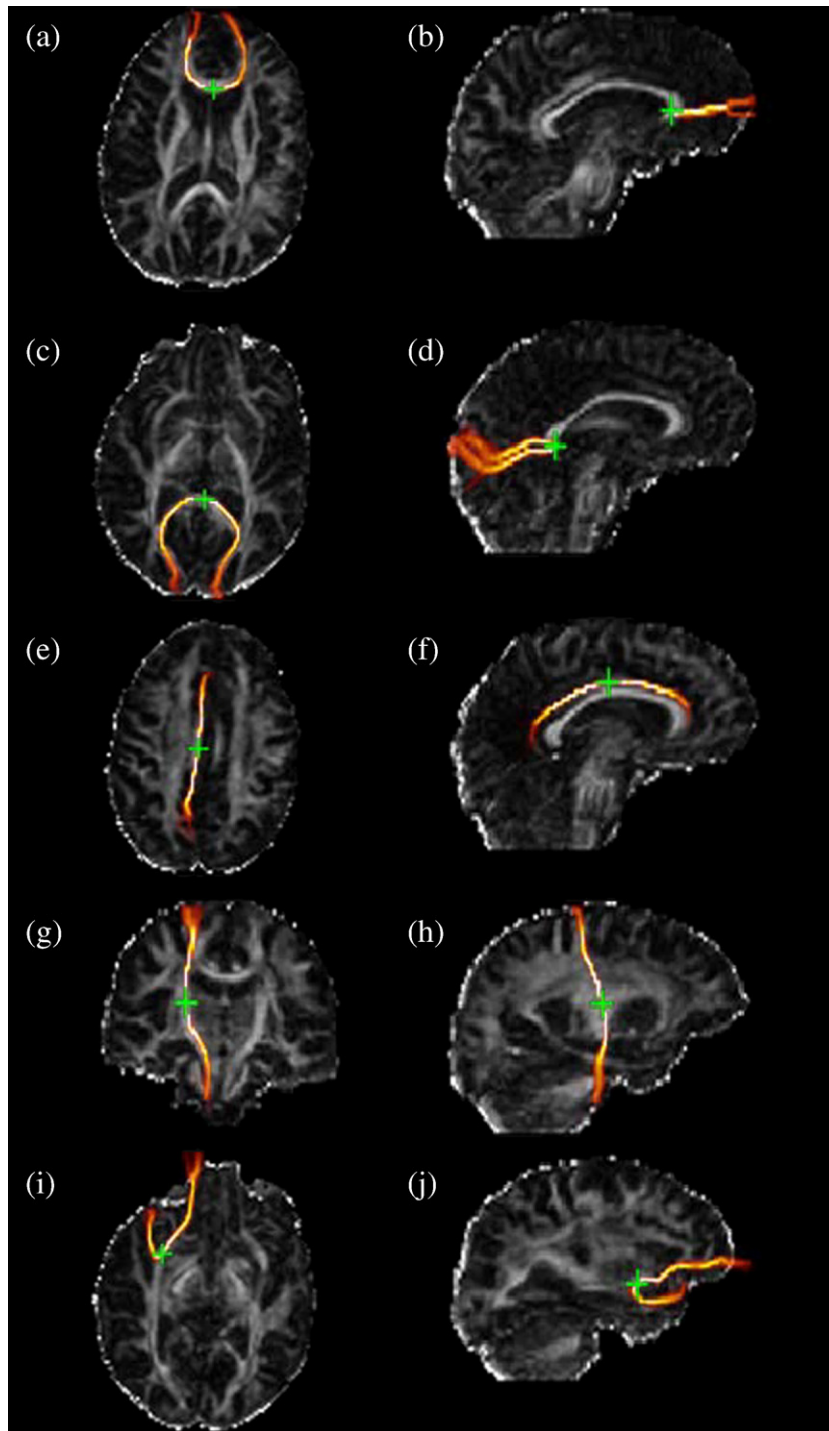


Fig. 3. Two-dimensional projections of the reference tracts for genu (first row), splenium (second row), right cingulum cingulate gyrus (third row), right corticospinal tract (fourth row) and right uncinate fasciculus overlaid on maps of FA. The green stars indicate the seed point locations corresponding to the MNI coordinates given in Table 1. The colours represent the proportion of probabilistic streamlines passing through each voxel, as indicated by the colour bar in Fig. 2.

Tractography analysis

The best match tracts produced by PNT and those segmented by transferring single seed points directly from standard to native space, which we will term the 'registration method', were assessed in several ways. First, tracts were visually inspected by a rater experienced with tractography (MEB) to establish whether or not they were anatomically plausible representations of the fasciculus-of-interest, and the number of acceptable tracts generated by each method counted. Specifically, tracts were deemed not to be acceptable if they were

heavily truncated, deviated significantly from their known anatomical orientation or had one or more branches heading into unrelated structures (see Fig. 4). The variation of tractography-based water diffusion measurements was then assessed by calculating tract-averaged values of $\langle D \rangle$ and FA for each fasciculus and determining the inter-subject CVs ($=SD/mean \times 100\%$) for the registration and PNT methods. The effects of normal ageing on white matter structure were investigated by correlating \mathbf{R} (Spearman's ρ), and tract-averaged $\langle D \rangle$ and FA (Pearson's r), measured for the best match tract with age for the eight fasciculi-of-interest. All statistical tests were performed

Table 1

Reference tract seed voxel MNI coordinates and mean (\pm SD) values for the log-ratio between the matching likelihood of the training tract and the matching likelihood of the reference tract (**R**) averaged over the tracts used to train the tract shape model for the eight fasciculi-of-interest

	Reference tract MNI coordinates (x, y, z)	R
Genu	0, 27, 1	-16.00 \pm 4.98
Splenium	-1, -42, 8	-21.13 \pm 5.07
Left CCG	-5, -2, 37	-27.08 \pm 7.26
Right CCG	7, -3, 37	-25.53 \pm 6.43
Left CST	-23, -11, 11	-18.94 \pm 3.99
Right CST	25, -14, 13	-29.23 \pm 5.70
Left uncinate	-33, 7, -12	-25.13 \pm 12.61
Right uncinate	35, 1, -14	-24.20 \pm 9.04

using SPSS 14.0 (SPSS Inc, Chicago, Ill, USA), with $p < 0.05$ being considered statistically significant.

Results

Table 1 shows the MNI coordinates for the reference tract seed voxels and **R** averaged over the tracts used to train the model for the eight fasciculi-of-interest. Values of **R** vary substantially from tract to tract, and range from approximately -16 for genu to -29 for right CST.

Comparison of acceptable tracts

The number of tracts visually assessed to be anatomically plausible representations of each of the eight fasciculi-of-interest generated by the registration and PNT methods is presented in Table 2. In all cases, the latter provides significantly more acceptable tracts than the former. For example, in the CCG the number of acceptable tracts produced by PNT ranges from 75 to 80%, compared with 12.5 to 17.5% for the registration method. This improvement is illustrated in Fig. 5, where two-dimensional sagittal projections of the right CCG produced by the registration and PNT methods are shown for six subjects aged between 70 and 80 years. Combining the output from both methods produces only a negligible increase in the number of acceptable tracts, indicating that the registration method does not provide many additional acceptable tracts to those identified by PNT. However, the number of subjects in which neither method can provide satisfactory tracts ranges from 7.5% in splenium to 30% in the left uncinate fasciculus.

To investigate whether **R** differs significantly between anatomically acceptable and unacceptable tracts, Table 3 shows average values of **R** for these two tract groups. For each fasciculus, **R** is always more negative for unacceptable than acceptable tracts, with these differences reaching statistical significance in the genu, CCG and left uncinate fasciculus when assessed with Mann-Whitney *U* tests. Furthermore, with the exception of right CST, the average value of **R** for acceptable tracts is very similar to those calculated when training the model. In splenium, for example, average **R** for the training data is -21.13 \pm 5.07, while **R** for the acceptable tracts is -21.70 \pm 6.20.

Coefficients-of-variation of tract-averaged diffusion parameters

Table 4 displays values of $\langle D \rangle$ and FA, and their associated CVs, for the registration and PNT methods in the eight fasciculi-of-interest. In general, there is a significant reduction, in some cases by half, in the CVs of $\langle D \rangle$ and FA measured using PNT compared with those measured using the registration method. In right CCG, for example, the CVs decrease from 16.8 to 6.4% for $\langle D \rangle$, and 28.8 to 15.6% for FA. This results from a significant reduction in the SD of the tract-averaged $\langle D \rangle$ and FA provided by PNT, coupled with a decrease in $\langle D \rangle$ and an increase in FA, as the tract profile more

faithfully and completely follows the underlying white matter fasciculi.

Correlations of **R** and diffusion parameters with age

Of the eight fasciculi investigated, only genu provided significant correlations between either **R** or tract-averaged diffusion parameters and age: **R** versus age ($\rho = -0.33$, $p = 0.04$; Fig. 6a), and FA versus age ($r = -0.41$, $p < 0.01$; Fig. 6b). Removing those tracts ($N = 7$) that were not anatomically acceptable representations of the genu produced: **R** versus age ($\rho = -0.36$, $p = 0.04$), and FA versus age ($r = -0.32$, $p = 0.06$).

Discussion

The contributions of this work are fourfold. Firstly, we have demonstrated that PNT is capable of segmenting a range of white matter structures in a group of normal ageing subjects, without there being the need to create 'old brain' reference tracts specifically for use with such a population. Second, the agreement between the subjective assessment of segmentation 'acceptability' and the objective log-ratio measure confirms that **R** can be a useful indicator of goodness-of-match to a specific reference tract. Third, we have used this log-ratio measure, which is unique to PNT, to find evidence suggesting that the topology of corpus callosum genu is significantly affected by the ageing process. Finally, we have reproduced the previously seen finding of a negative correlation between FA and age, again specific to the genu.

Tractography has the unique potential to map the brain's circuitry *in vivo* and provide detailed information on how cerebral structure correlates with function and dysfunction in health and disease. In cross-sectional studies, however, this potential can only be fully realised if the same tract is reliably identified in each participant. In the present work, we show the application of a novel method for automatic seed point placement that aims to segment the same tract from subject to subject in a group of normal older volunteers. For the eight fasciculi investigated, the results show that it is possible to use single seed point tractography to identify the same tract in approximately 70 to 90% of ageing subjects depending on the tract in question. This is a significantly greater percentage than that afforded by simply registering seed points directly from standard to native space. It might be argued that the latter approach is rarely used in practice, with those studies that use single seed point tractography more typically placing the seed point by hand in regions of high diffusion anisotropy (Ciccarelli et al., 2003; Heiervang et al., 2006); but its automated nature and observer independence, in common with PNT, makes for a useful comparison. An alternative approach is provided by seeding from a cluster of voxels within a volume-of-interest, with the tractography algorithm run either unconstrained or constrained by waypoint ROIs, and combining the resulting tract data (Conturo et al., 1999; Heiervang et al., 2006; Wakana et al., 2007). Using a multiple ROI method with masks defined in standard space and the same underlying probabilistic tractography algorithm as employed here, Heiervang et al. (2006) measured CVs in the range 1.4 to 4.9 and 3.3 to 9.3% for $\langle D \rangle$ and FA in genu, pyramidal tract and CCG in a group of eight healthy volunteers aged 21 to 34 years. Given the wide age range of our elderly cohort, varying degrees of brain atrophy and evidence for progressive change in diffusion parameters with age in the genu, the CVs for PNT $\langle D \rangle$ and FA (Table 4) compare well with these results. In contrast to multiple ROI methods, PNT has the advantage that the tractography algorithm can be run unconstrained without complicated target, termination or exclusion masks, thereby making the results less dependent on the preconceived expectations of the observer. A priori anatomical information does, of course, remain in PNT, albeit in the subtler guise of the reference tract and training data.

Although PNT is able to generate a far greater number of anatomically convincing tracts than the registration method in this

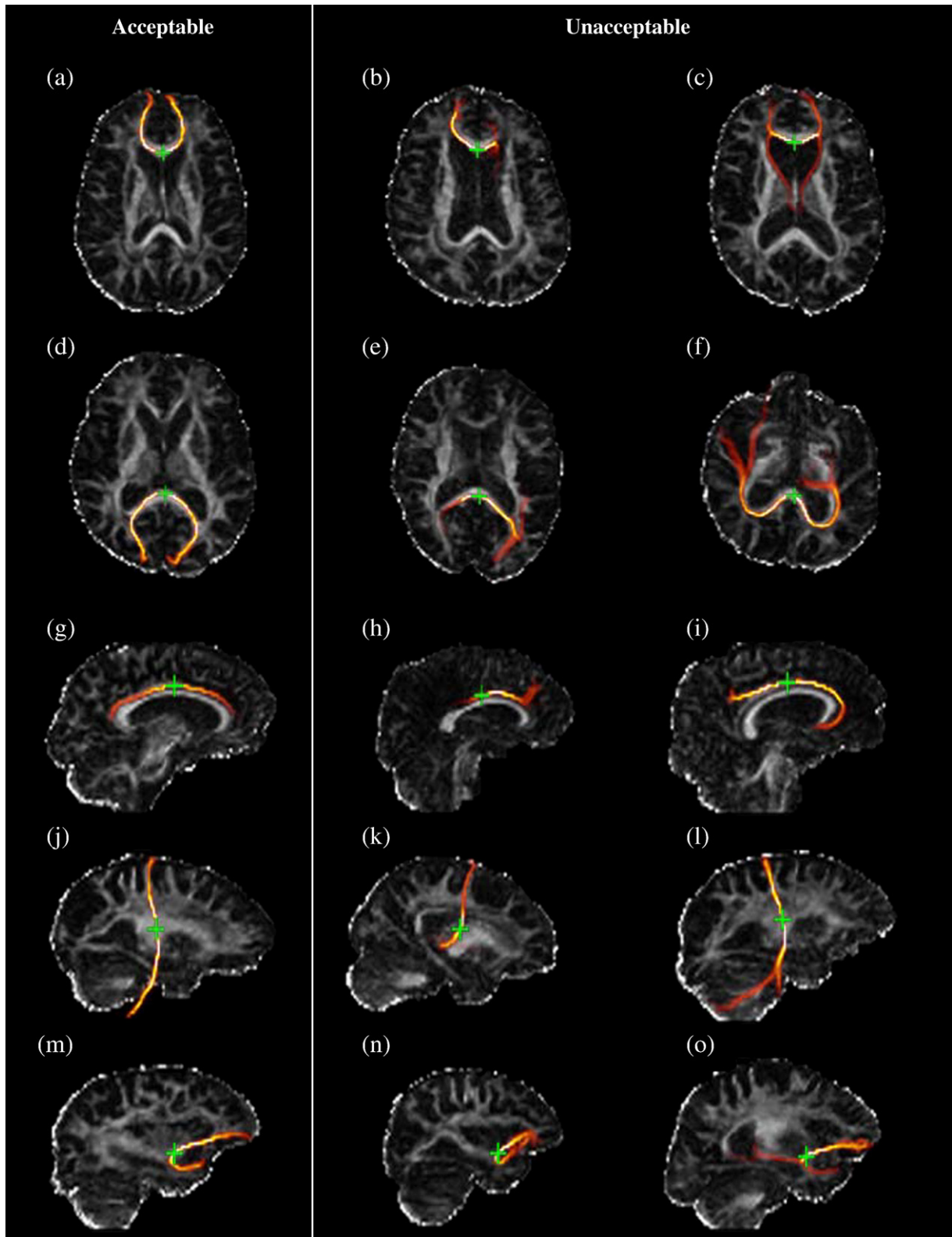


Fig. 4. Examples of tracts that were considered anatomically acceptable and unacceptable representations of genu (first row), splenium (second row), cingulum cingulate gyri (third row), corticospinal tracts (fourth row) and uncinate fasciculi overlaid on maps of FA. The colours represent the proportion of probabilistic streamlines generated from the seed point (green star) passing through each voxel, as indicated by the colour bar in Fig. 2.

ageing cohort, in a number of subjects it is still unable to provide acceptable tracts. This varies from 10% in splenium to 25% in right CCG and 30% in left uncinate fasciculus. Given that PNT is entirely dependent on the quality of the underlying tractography data, this is

perhaps to be expected since splenium is a large white matter structure, while the CCG are smaller and more prone to partial volume averaging and the uncinate fasciculi are close to the inferior longitudinal fasciculi. (Heiervang et al. (2006) also found that in the

Table 2
The percentage of subjects in whom tracts generated by the registration and PNT methods were considered anatomically acceptable representations of the fasciculus-of-interest

%	Genu	Splenium	Left CCG	Right CCG	Left CST	Right CST	Left uncinate	Right uncinate
Registration method acceptable	60	32.5	12.5	17.5	10	2.5	15	15
PNT acceptable	82.5	90	80	75	77.5	80	70	85
Either acceptable	85	92.5	82.5	75	80	82.5	70	90
Neither acceptable	15	7.5	17.5	25	20	17.5	30	10

four tracts they investigated diffusion measures were most variable in CCG.) In practice, however, a significant number of the discarded tracts were deemed unacceptable not because the main trajectory of the tract was incorrect, but because there were one or more branches heading into unrelated structures, e.g. Fig. 4 (c, l, o). In left uncinate fasciculus, for example, this was the reason for rejecting 10 of the 12

subjects with unacceptable tracts. Since the aim of the method is to segment the same tract reliably in different subjects, this is a stringent, but appropriate criterion for rejection. Raising the level at which the tractography mask is thresholded, currently set at 1%, will reduce more of these branching structures and hence potentially increase the number of acceptable tracts, albeit with a concomitant reduction in

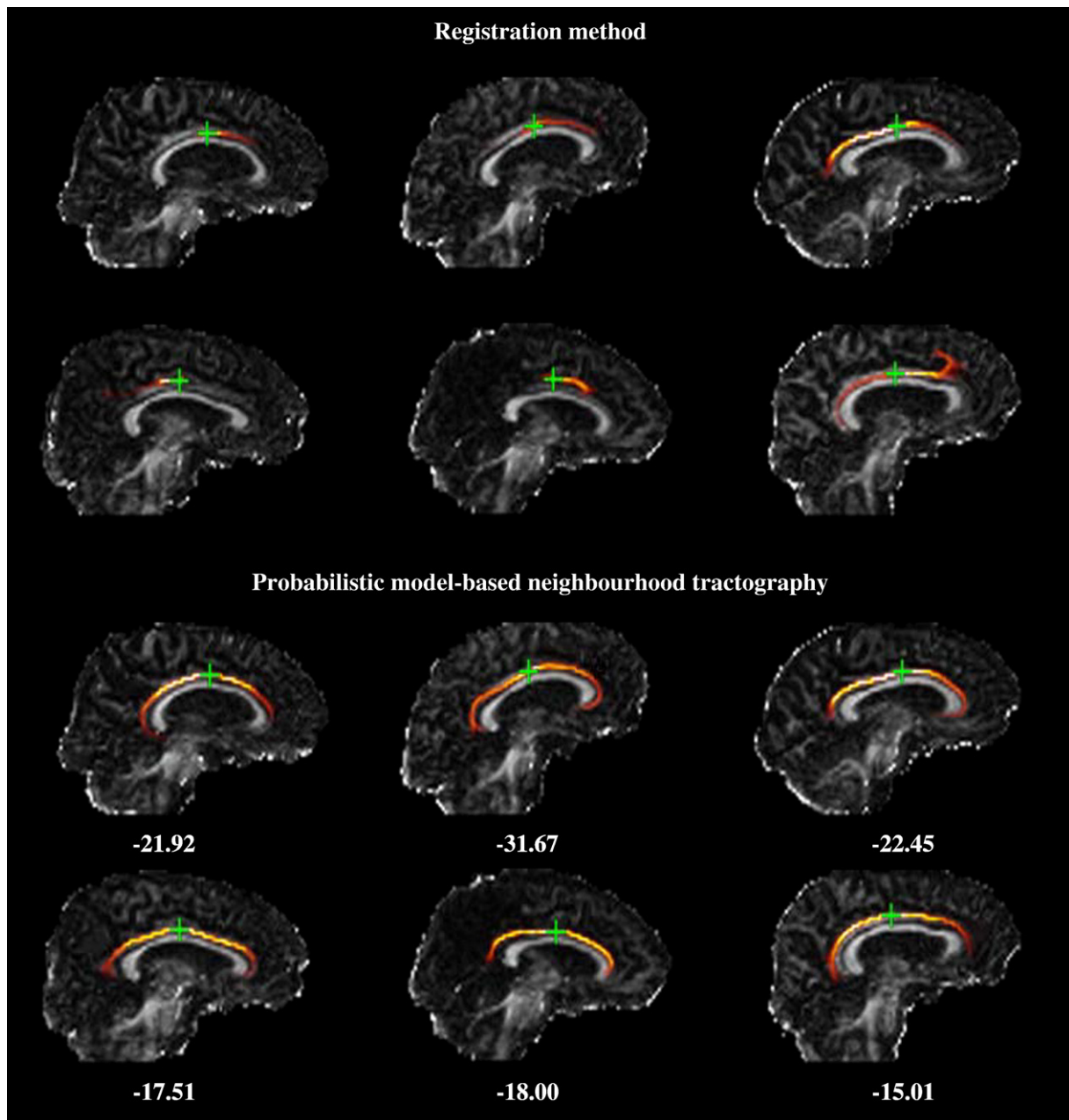


Fig. 5. Two-dimensional sagittal projections of the right cingulum cingulate gyrus obtained using the registration and PNT methods in six subjects aged between 70 and 80 years of age overlaid on maps of FA. For PNT, values of R are given for each subject. The colours represent the proportion of probabilistic streamlines generated from the seed point (green star) passing through each voxel, as indicated by the colour bar in Fig. 2.

Table 3

Mean (\pm SD) values for the log-ratio between the matching likelihood of the best match tract and the matching likelihood of the reference tract (**R**) for those tracts that were considered anatomically acceptable or unacceptable representations of the fasciculus-of-interest

R	Acceptable	Unacceptable
Genu	-20.14 \pm 10.29	-33.37 \pm 16.52
Splenium	-21.70 \pm 6.20	-30.39 \pm 14.13
Left CCG	-28.10 \pm 9.57	-38.12 \pm 11.97
Right CCG	-29.73 \pm 11.28	-58.98 \pm 20.20
Left CST	-16.24 \pm 7.29	-21.78 \pm 9.86
Right CST	-21.92 \pm 8.06	-27.79 \pm 12.58
Left uncinate	-20.41 \pm 9.17	-28.16 \pm 10.33
Right uncinate	-18.41 \pm 4.26	-21.63 \pm 3.92

Bold type indicates a significant difference ($p < 0.05$) between **R** measured in acceptable and unacceptable tracts as assessed by the Mann-Whitney *U* test.

the mask volume of the main portion of the tract and truncation of distal parts of the tract.

A unique capability of PNT is that it provides a quantitative measure of how well the best match tract mirrors the reference tract, namely **R**. Although **R** is calculated relative to the appropriate reference tract and so values are not meaningful across fasciculi, Table 3 shows that it is always more negative for anatomically unacceptable than acceptable tracts. It is therefore a useful indicator of whether a tract is likely to be acceptable or not. Of particular interest, though, is the observation that **R** has a significant negative correlation with age in corpus callosum genu. This result indicates that the best match tract tends topologically to deviate more markedly from the genu reference as the subject's age increases. Given that the reference subject is a 31 year old, and the genu follows the edge of the lateral ventricles which tend to enlarge with age, perhaps this result might be considered unsurprising. However, there was no significant negative correlation between **R** and age in the splenium in this cohort, suggesting that these topological changes are more localised in frontal regions. This view is supported by the results of Sullivan et al. (2006) who used quantitative tractography to investigate age-related deterioration of anterior callosal fibres in 10 older (72 ± 5 years) and 10 younger (29 ± 5 years) subjects. Seeding from regions based on known callosal anatomical projections within the mid-sagittal corpus callosum, they found that the older group of subjects had significantly shorter anterior callosal fibre bundles than the younger group in the most anterior callosal fibre bundles. Additional studies using other techniques, such as deformation-based morphometry which can provide quantitative maps of brain volume changes relative to a reference atlas (Cardenas et al., 2007), are now needed to confirm this finding and elucidate further the structural changes that accompany normal ageing.

The observation that genu FA has a near significant negative correlation with age, while no other similar correlations are present in the other fasciculi investigated, provides further evidence that age-related structural changes may be affecting this tract. These findings appear consistent with the 'frontal ageing' hypothesis which posits that there is an approximately anterior-to-posterior gradient in white matter structural deterioration with age (O'Sullivan et al., 2001; Head

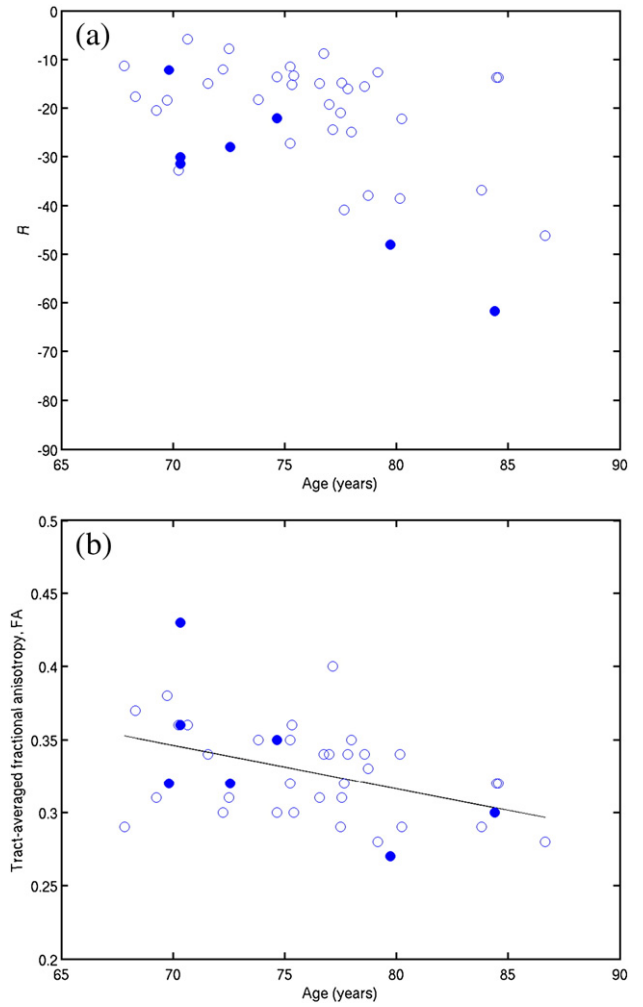


Fig. 6. Plots of **R** (a) and tract-averaged FA (b) versus age for corpus callosum genu. Closed circles indicate subjects whose tracts that were deemed to be anatomically unacceptable representations of the fasciculus-of-interest.

et al., 2004; Pfefferbaum et al., 2005; Sullivan et al., 2006). This hypothesis is supported by a large number of ROI studies which have shown a significant decrease in FA with advancing age, a trend that is greater in the genu than the splenium (Abe et al., 2002; Salat et al., 2005; Sullivan and Pfefferbaum, 2006). Using tract-based spatial statistics, Kochunov et al. (2007) found that genu FA had a more robust association with other indices of brain structural health, such as whole brain grey matter thickness and white matter lesion volume, than did FA measured in other white matter regions, again indicating the predisposition of this tract to degenerative change in ageing. Sullivan et al. (2006) also measured significantly lower FA in the three most frontal callosal fibre bundles they investigated using quantitative

Table 4

Mean (\pm SD) values and coefficients-of-variation (CV) for mean diffusivity ($\langle D \rangle$) and fractional anisotropy (FA) in the eight fasciculi-of-interest generated by the registration and PNT methods

Method	Genu		Splenium		Left CCG		Right CCG		Left CST		Right CST		Left uncinate		Right uncinate	
	Mean	CV (%)														
$\langle D \rangle$ Registration	1072 \pm 180	16.8	954 \pm 146	15.3	970 \pm 164	16.9	901 \pm 151	16.8	905 \pm 83	9.2	912 \pm 93	10.2	996 \pm 167	16.8	944 \pm 92	9.7
PNT	1007 \pm 74	7.4	941 \pm 85	9.0	856 \pm 63	7.4	826 \pm 53	6.4	915 \pm 84	9.2	882 \pm 89	10.0	959 \pm 63	6.6	953 \pm 59	6.2
FA Registration	0.32 \pm 0.04	12.3	0.38 \pm 0.04	10.2	0.26 \pm 0.08	29.3	0.28 \pm 0.08	28.8	0.42 \pm 0.04	10.2	0.41 \pm 0.04	9.1	0.29 \pm 0.06	22.1	0.35 \pm 0.05	14.2
PNT	0.33 \pm 0.03	10.2	0.39 \pm 0.04	9.4	0.31 \pm 0.04	12.8	0.31 \pm 0.05	15.6	0.43 \pm 0.03	7.6	0.44 \pm 0.03	7.5	0.31 \pm 0.04	12.5	0.30 \pm 0.03	8.7

The units of $\langle D \rangle$ are $\times 10^{-6}$ mm²/s.

tractography. Interestingly, however, while these studies often report a significant increase in $\langle D \rangle$ with age in genu, we did not find such an association. We also did not find significant correlations between diffusion parameters and age in the uncinate fasciculi which have a significant frontal lobe component. Thus, although our FA results fit into the broad current of these studies, further work is required to confirm that tractography-based measurements support the ‘frontal ageing’ hypothesis and fully agree with the wealth of ROI and other imaging-based data.

A potential weakness of the method in its current form is the definition of the reference tract from a single individual and the need to use separate training data to fit parameters to the model. For this study we used tract data from a group much younger than the main cohort to accentuate potential structural differences between young and old brains, and to demonstrate the portability of reference tracts between groups. However, to investigate whether the above results are critically dependent on the specific form of the reference tract and training data, a further set of 15 subjects aged between 66 and 80 years were recruited, and a new model generated using reference tract and training data taken from this additional group. Even given small differences in the location of the reference tract seed points, the results of this new model were very similar to those presented above, indicating a reasonable degree of robustness of the method to different initialization conditions. (In genu, for example, 82.5% of tracts generated using PNT were acceptable representations of the fasciculus, compared with 47.5% for the registration method. Again, R ($\rho = -0.55$, $p < 0.001$) and FA ($r = -0.37$, $p = 0.02$) had significant correlations with age for the 40 subjects. Removing those subjects whose tracts were not anatomically acceptable representations of the genu ($N = 7$) produced: R versus age ($\rho = -0.58$, $p < 0.001$), and FA versus age ($r = -0.33$, $p = 0.06$). As above there were no other significant correlations between these parameters in the other fasciculi studied). Nevertheless, we are currently working on enhancements to make the method still more objective. For example, reference tracts can be made independent of any dataset by defining them using a published human white matter atlas (Muñoz Maniega et al., 2008), while it is possible to train the model with data from the (200 plus) candidate tracts themselves rather than a small group of separate hand picked training tracts using an “unsupervised learning” technique (Clayden, 2008). The utility of these additions is currently under investigation will form the basis of future studies.

In summary then, these data show that PNT is capable of automatically segmenting comparable tracts in the brains of normal ageing subjects. The advantage of the NT approach is that the specificity of single seed point tractography is retained, while the undesirable sensitivity to precise seed point placement is mitigated. This allows the tractography algorithm to be run unconstrained without complicated target, termination or exclusion masks, as required in multiple ROI methods. We have also demonstrated evidence of topological change as well as potential loss of integrity (as indicated by reduced FA) with age, specific to the corpus callosum genu. It is quite possible that the systematic declines in R and FA are linked to a single underlying process, but beyond general brain atrophy it is not clear what precisely this process might be. Our findings with regard to topology should be treated as tentative at this stage, and need to be reproduced, but our study supports the view that frontal white matter, in particular corpus callosum genu, may be preferentially and adversely altered during the course of normal ageing.

Acknowledgments

This work was partly supported by an MRC Clinician Scientist Fellowship for AMJM. JPP and JDC have been supported by an EPSRC/MRC studentship via the Neuroinformatics Doctoral Training Centre, University of Edinburgh. We acknowledge the support of the MRC Centre for Cognitive Ageing and Cognitive Epidemiology. All MRI data

were collected at the SFC Brain Imaging Research Centre, University of Edinburgh (<http://www.dcn.ed.ac.uk/bic>).

References

- Abe, O., Aoki, S., Hayashi, N., Yamada, H., Kunimatsu, A., Mori, H., Yoshikawa, T., Okubo, T., Ohtomo, K., 2002. Normal aging in the central nervous system: quantitative MR diffusion-tensor analysis. *Neurobiol. Aging* 23, 433–441.
- Armstrong, C.L., Traipe, E., Hunter, J.V., Haselgrove, J.C., Ledakis, G.E., Tallent, E.M., Shera, D., van Buchem, M.A., 2004. Age-related, regional, hemispheric, and medial-lateral differences in myelin integrity in vivo in the normal adult brain. *AJNR Am. J. Neuroradiol.* 25, 977–984.
- Bartzokis, G., Cummings, J.L., Sultzer, D., Henderson, V.W., Nuechterlein, K.H., Mintz, J., 2003. White matter structural integrity in healthy aging adults and patients with Alzheimer disease: a magnetic resonance imaging study. *Arch. Neurol.* 60, 393–398.
- Behrens, T.E., Woolrich, M.W., Jenkinson, M., Johansen-Berg, H., Nunes, R.G., Clare, S., Matthews, P.M., Brady, J.M., Smith, S.M., 2003. Characterization and propagation of uncertainty in diffusion-weighted MR imaging. *Magn. Reson. Med.* 50, 1077–1088.
- Cardenas, V.A., Boxer, A.L., Chao, L.L., Gorno-Tempini, M.L., Miller, B.L., Weiner, M.W., Studholme, C., 2007. Deformation-based morphometry reveals brain atrophy in frontotemporal dementia. *Arch. Neurol.* 64, 873–877.
- Ciccarelli, O., Parker, G.J., Toosy, A.T., Wheeler-Kingshott, C.A., Barker, G.J., Boulby, P.A., Miller, D.H., Thompson, A.J., 2003. From diffusion tractography to quantitative white matter tract measures: a reproducibility study. *NeuroImage* 18, 348–359.
- Clayden, J.D., 2008. Comparative analysis of connection and disconnection in the human brain using diffusion MRI: new methods and applications. PhD Thesis, University of Edinburgh.
- Clayden, J.D., Bastin, M.E., Storkey, A.J., 2006. Improved segmentation reproducibility in group tractography using a quantitative tract similarity measure. *NeuroImage* 33, 482–492.
- Clayden, J.D., Storkey, A.J., Bastin, M.E., 2007. A probabilistic model-based approach to consistent white matter tract segmentation. *IEEE Trans. Med. Imaging* 26, 1555–1561.
- Conturo, T.E., Lori, N.F., Cull, T.S., Akbudak, E., Snyder, A.Z., Shimony, J.S., McKinstry, R.C., Burton, H., Raichle, M.E., 1999. Tracking neuronal fiber pathways in the living human brain. *Proc. Natl. Acad. Sci. U.S.A.* 96, 10422–10427.
- Evans, A.C., Collins, D.L., Mills, S.R., Brown, E.D., Kelly, R.L., Peters, T.M., 2003. 3D statistical neuroanatomical models from 305 MRI volumes. *Proc. IEEE Nucl. Sci. Symp. Med. Imag. Conf.* 95, 1813.
- Geschwind, N., 1965. Disconnection syndromes in animals and man. *Brain* 88, 237–294.
- Greenwood, P.M., 2000. The frontal aging hypothesis evaluated. *J. Int. Neuropsychol. Soc.* 6, 705–726.
- Head, D., Buckner, R.L., Shimony, J.S., Williams, L.E., Akbudak, E., Conturo, T.E., McAvoy, M., Morris, J.C., Snyder, A.Z., 2004. Differential vulnerability of anterior white matter in nondemented aging with minimal acceleration in dementia of the Alzheimer type: evidence from diffusion tensor imaging. *Cereb. Cortex* 14, 410–423.
- Heiervang, E., Behrens, T.E., Mackay, C.E., Robson, M.D., Johansen-Berg, H., 2006. Between session reproducibility and between subject variability of diffusion MR and tractography measures. *NeuroImage* 33, 867–877.
- Hua, K., Zhang, J., Wakana, S., Jiang, H., Li, X., Reich, D.S., Calabresi, P.A., Pekar, J.J., van Zijl, P.C., Mori, S., 2008. Tract probability maps in stereotaxic spaces: analyses of white matter anatomy and tract-specific quantification. *NeuroImage* 39, 336–347.
- Jenkinson, M., Smith, S., 2001. A global optimisation method for robust affine registration of brain images. *Med. Image Anal.* 5, 143–156.
- Jones, D.K., Williams, S.C., Gasston, D., Horsfield, M.A., Simmons, A., Howard, R., 2002. Isotropic resolution diffusion tensor imaging with whole brain acquisition in a clinically acceptable time. *Hum. Brain Mapp.* 15, 216–230.
- Kochunov, P., Thompson, P.M., Lancaster, J.L., Bartzokis, G., Smith, S., Coyle, T., Royall, D.R., Laird, A., Fox, P.T., 2007. Relationship between white matter fractional anisotropy and other indices of cerebral health in normal aging: tract-based spatial statistics study of aging. *NeuroImage* 35, 478–487.
- Muñoz Maniega, S., Bastin, M.E., McIntosh, A.M., Lawrie, S.M., Clayden, J.D., 2008. Atlas-based reference tracts improve automatic white matter segmentation with neighbourhood tractography. *Proc. Intl. Soc. Magn. Reson. Med.* 16, 3318.
- O’Sullivan, M., Jones, D.K., Summers, P.E., Morris, R.G., Williams, S.C., Markus, H.S., 2001. Evidence for cortical “disconnection” as a mechanism of age-related cognitive decline. *Neurology* 57, 632–638.
- Pfefferbaum, A., Adalsteinsson, E., Sullivan, E.V., 2005. Frontal circuitry degradation marks healthy adult aging: evidence from diffusion tensor imaging. *NeuroImage* 26, 891–899.
- Pierpaoli, C., Jezzard, P., Basser, P.J., Barnett, A., Di Chiro, G., 1996. Diffusion tensor MR imaging of the human brain. *Radiology* 201, 637–648.
- Salat, D.H., Tuch, D.S., Greve, D.N., van der Kouwe, A.J., Hevelone, N.D., Zaleta, A.K., Rosen, B.R., Fischl, B., Corkin, S., Rosas, H.D., Dale, A.M., 2005. Age-related alterations in white matter microstructure measured by diffusion tensor imaging. *Neurobiol. Aging* 26, 1215–1227.
- Sullivan, E.V., Pfefferbaum, A., 2006. Diffusion tensor imaging and aging. *Neurosci. Biobehav. Rev.* 30, 749–761.
- Sullivan, E.V., Adalsteinsson, E., Pfefferbaum, A., 2006. Selective age-related degradation of anterior callosal fiber bundles quantified in vivo with fiber tracking. *Cereb. Cortex* 16, 1030–1039.
- Wakana, S., Caprihan, A., Panzenboeck, M.M., Fallon, J.H., Perry, M., Gollub, R.L., Hua, K., Zhang, J., Jiang, H., Dubey, P., Blitz, A., van Zijl, P., Mori, S., 2007. Reproducibility of quantitative tractography methods applied to cerebral white matter. *NeuroImage* 36, 630–644.